Article

Accounting for Carbon Sink and Its Dominant Influencing Factors in Chinese Ecological Space

Gang Lin [1,2], Dong Jiang [1,2,3], Xiang Li [4,*] and Jingying Fu [1,2,*]

1   Institute of Geographic Sciences and Natural Resources Research, Chinese Academy of Sciences, Beijing 100101, China
2   College of Resources and Environment, University of Chinese Academy of Sciences, Beijing 100049, China
3   Key Laboratory of Carrying Capacity Assessment for Resource and Environment, Ministry of Natural Resources, Beijing 100812, China
4   College of Geoscience and Surveying Engineering, China University of Mining & Technology-Beijing, Beijing 100083, China
*   Correspondence: lx@student.cumtb.edu.cn (X.L.); fujy@igsnrr.ac.cn (J.F.); Tel.: +86-18600019687 (X.L.)

Abstract: Ecological space (ES), including forest ecological space (FES) and grassland ecological space (GES) in this study, is the land with natural attributes and the main functions of providing ecological services, which has a huge potential capacity for carbon sink (CS). The interannual fluctuation of the CS in ES is severe, which is affected by factors such as precipitation and temperature, but it is still controversial which is the dominant factor in affecting the fluctuation process of the CS in ES. To this end, the multi-source remote sensing monitoring data on the fine-grid scale were collected in this study, including the land use and land cover remote sensing monitoring data, the data products of moderate-resolution imaging spectroradiometer (including land surface water index, photosynthetically active radiation, enhanced vegetation index, gross primary productivity), and meteorological data (including precipitation and temperature). By coupling the vegetation photosynthesis model and soil respiration model, the CS in CES from 2010 to 2020 was calculated, and the interannual fluctuation trends and stability of CS in CES were analyzed. Furthermore, the correlation coefficient and partial correlation coefficient equation between the CS of CES with precipitation and temperature were constructed to explore the correlation between interannual fluctuation of CS in CES with meteorological factor, and to determine the dominant position of precipitation and temperature in affecting the fluctuation process of the CS in CES. The research results show that the annual average CS of per unit area in CES was 233.78 $gC \cdot m^{-2} \cdot a^{-1}$, and the cumulative CS was 11.83 PgC. The GES and FES contributed 6.33 PgC and 5.49 PgC of CS, respectively. From 2010 to 2020, the CS of CES showed an upward trend and was generally in a relatively stable state (the mean value of the coefficient of variation was 0.6248). However, the year with severe fluctuation of was found in this study (from 2013 to 2015), the reason is that the precipitation was too low in 2014, which indicated that climate change, especially the change of precipitation, played a important role in the fluctuation of CS in CES. The results of correlation analysis confirmed the above analysis. The change of CS in CES is highly positively correlated with the change of precipitation (the correlation coefficient is 0.085), and weakly positively correlation with temperature (the correlation coefficient was 0.026). The precipitation is the dominant influencing factor, which has a positive effect on CS in CES. Within a climate environment dominated by precipitation, precipitation and temperature jointly affect the CS in CES. It should be noted that in some regions with variable climate, precipitation and temperature had relatively little impact on CS in CES. Their fluctuations may depend more on the ecosystem's own ecological services' regulation ability and their response degree to changes in atmospheric CO_2 concentration.

Keywords: ecological space; net ecosystem productivity; carbon sink; carbon peak and neutrality

1. Introduction

The development of economic globalization in the 21st century has led to the rapid growth of population and vice versa. This has been followed by a surge in and the unreasonable utilization of energy resources and land resources, which has led to a sharp increase in greenhouse gases such as CO_2 and frequent global climate change events such as global warming and extreme climate [1–4]. The problem of how to effectively deal with climate change, reduce excessive CO_2 emissions, and solve the increasingly prominent climate problem is an important direction of the current scientific research and is also the goal of the joint efforts of all governments [5–9]. In September 2020, the Chinese government pledged at the United Nations General Assembly to "strive to achieve a carbon peak by 2030 and achieve carbon neutrality by 2060", which means that by 2060, China's carbon emissions will be reduced from the current amount—near 10 billion tons per year—to "nearly zero" emissions [10]. To this end, China has introduced a series of policies and regulations to fully support the realization of the carbon peak and neutrality ("dual carbon" goals) [7,8,11]. In general, China will achieve carbon neutrality in two ways: One is to reduce carbon emissions through renewable energy utilization and the development of energy-saving technologies [12–15]. The second is to reduce CO_2 in the atmosphere by improving carbon sink (CS) in the ecosystem and developing technologies of CS [16–18].

Ecological space (ES) is the land with natural attributes and the main functions of providing ecological services or ecological products [19]. In this study, the ES includes forest ecological space (FES) and grassland ecological space (GES), which has a huge potential capacity of CS [20–22]. According to the Global Carbon Project, the global ES net absorbed 31% of the CO_2 released by human activities in the same period from 2010 to 2019 [23]. Therefore, improving the quality and stability of ES and optimizing the ES should not only be limited to optimizing the layout of ES through afforestation but also be reflected in optimizing the ecological service value of ES and consolidating and upgrading the function of CS in ES. For China, the carbon peak by 2030 and carbon neutrality by 2060 have become important long-term strategic goals [10]. Therefore, it is necessary to coordinate the macro layout of emission reduction, carbon sink increase and carbon sequestration, promote the low-carbon transformation of industrial structure, improve the increment of CS in ES, and develop key carbon sequestration technologies, which are important ways and necessary measures for China to achieve the "dual carbon" goals [24]. Inevitably, the realization of these technologies and measures must rely on the huge potential reserves of CS in Chinese ecological space (CES). Therefore, for China, the current primary task is to protect the ES, establish an accurate accounting method for CS, find out the background amount of CS in CES, and evaluate the stability and sustainability of CS.

When searching for "ecosystem" and "net ecosystem productivity (NEP), a total of 3197 related articles were published from 2018 to 2022 on Web of Science. The vocabulary of these articles mainly includes topics in the study of "ecosystem", "climate change", "carbon cycle", "forests", "grassland", etc. This indicates that the carbon cycle and CS of ES are attracting unprecedented attention with major national demands such as the construction of ecological civilization and "dual carbon" goals of China. On the global scale, Wang et al. [25] used multi-scale remote sensing monitoring and inversion data, combined with the atmospheric inversion method, ecosystem carbon cycle model and machine learning model, to generate a $1° \times 1°$ global terrestrial carbon flux dataset, discussed the mechanism of interannual variation in the global CS, and the impact of temperature and water changes on global terrestrial carbon sink in space the influence of temperature and water on the global CS in space. they thought that it is necessary to pay more attention to the differential effects of temperature change on the global terrestrial CS in the Northern Hemisphere to reveal the interannual variation therein. On the national scale, Zhang et al. [26] used eddy covariance measurement to measure the NEP and gross primary productivity (GPP) of three typical grasslands in China, and analyzed the characteristics and driving forces of their interannual dynamic changes. Their research results show that both climatic

factors such as temperature and precipitation, and ecosystem responses affected the inter-annual variation in grassland carbon fluxes. On the daily scale, carbon fluxes were mainly driven by climate factors, while on the annual scale, ecosystem responses weakened the effects of climate variability on carbon fluxes in the three grasslands. On the regional scale, Liu et al. [27] used the soil respiration model and the improved Carnegie–Ames–Stanford approach model, estimated the vegetation NEP in Qinghai Plateau from 2000 to 2015 based on remote sensing data and analyzed the interannual dynamic variation characteristics and influencing factors of vegetation NEP. Their research results show that the annual NEP of Qinghai Plateau was gradually improved and became stable, precipitation and temperature jointly affect the change of vegetation NEP in Qinghai Plateau. The average correlation coefficient between vegetation NEP and precipitation in Qinghai Plateau is 0.075, and precipitation mainly promoted the vegetation NEP; the average correlation coefficient between vegetation NEP and temperature in Qinghai Plateau is –0.20, and temperature mainly inhibited vegetation NEP.

Although the above studies provide a wide range of ideas and methods for the assessment and quality improvement of CS in ES, the following problems remain to be solved. For the study area and scale, current studies have focused on the global to regional scale, but they either study the common problems in large regions from a macro perspective or analyze the characteristics of CS in ES from a small regional perspective. The total area of Chinese ecological space (CES) is about 5.48 million km^2, accounting for 57.13% of the total area of China [28]. With such a large area proportion, the potential of CS in CES is bound to be very large, and there are also large interannual fluctuation characteristics and regional differences. However, there is no research on the accurate accounting of the interannual CS at the fine-grid scale in CES, and there is a lack of analysis of the spatial and temporal evolution characteristics of the whole region based on the grid data and the horizontal comparison of the CS at the provincial scale. As a result, there is still a great debate on the causes and mechanisms of the sharp interannual fluctuation of CS in ES. Therefore, a fine-grid scale accounting of CS in CES is necessary and urgently needed, which is of great significance when assessing CS in CES, exploring its fluctuation and change rules and formulating precise optimization and quality improvement policies to promote the realization of the "dual carbon" goals.

For the research content, it is well known that CS in ES are jointly affected by climate conditions such as temperature and precipitation, and the internal structure and process of ES are changed due to climate change. The CES spans five temperature zones, resulting in great differences in climatic conditions in the whole region, and it is these changes that affect the fluctuations of CS in CES. Although current studies have explored the relationship between CS in ES and climate change, we are concerned with determining the impact of temperature and precipitation on CS in CES under a more refined accounting system as well as finding out which factor plays a dominant role in promoting the differential change of ES in China. In addition, differences in climate conditions also manifested difference in the distribution of CES. The FES is mainly located in the southeast of China, and the GES is mainly located in the northwest of China. How does this distribution affect the overall CS in CES? How much difference is there in the capacity of CS between FES and GES? How much CS do they contribute for CES? These questions are also insufficiently addressed in the current studies.

Based on the above analysis, this study combined the vegetation photosynthesis model (VPM) and soil respiration model to establish an accounting method of CS on the grid scale. The model comprehensively considers vegetation photosynthesis, soil respiration, temperature, and precipitation, and then, the interannual variation trend and spatio-temporal stability of CS in CES from 2010 to 2020 were analyzed, and the influence of temperature and precipitation on the spatio-temporal variation of CS in CES from 2010 to 2020 was quantitatively analyzed in this study. The purpose of this study is to generate the spatial distribution data of CS in CES at the grid scale from 2010 to 2020, to more accurately understand and assess the status and potential of CS in CES at the fine-grid scale, to analyze

the fluctuation characteristics of CS in different regions of China, especially the differences of CS between FES and GES, and to determine the dominant factors of the annual change of CES. The data and conclusions obtained in this study will be welcomed by government policy-makers and scholars in the field of CS in ES.

This study is of significance for accurately understanding the potential of CS in CES, estimating the future changes of CO_2 concentration in the atmosphere, and accurately formulating effective policies to optimize ES quality and improve the capacity of CS according to the differences in ES.

2. Study Area and Data

2.1. Study Area

The distribution of CES is centralized and extensive. According to the data of China's Third National Land Survey, China has a total forest area of 2.84 million km^2 and grassland area of 2.64 million km^2 [28], The area proportion of FES and GES in different provinces is shown in Figure 1. The total area of FES and GES account for 57.13% of the total Chinese land area, which makes the CES carbon sink a feasible means for China and the world to cope with climate change and realize sustainable development. In terms of spatial distribution, the FES and GES are generally separated by the Heihe–Tengchong Line (also known as Hu Line, is the boundary line proposed by Hu [29] in 1935 to reveal the laws of population distribution in China [30]. It is highly coincident with 400 mm isohyet of China, which is the product of China's climate change and the dividing line of China's ecological environment.). The FES is mainly distributed in the east and southeast of China, while the GES is mainly distributed in the west and northwest of China (Figure 2). This is determined by the climate environment in China, and the distribution characteristics are caused by the climate differences between the two sides of the Heihe–Tengchong Line. For FES, the main resource types include coniferous forests, mixed coniferous and deciduous broad-leaved forests, broad-leaved forests, and so on [31]. The main resource types of GES are grassland and meadow [32]. The complex resource types lead to the large interannual fluctuation in CS in CES. As a result, the CS in CES is more significantly affected by temperature, precipitation, and other factors, showing obvious differences in spatial distribution. As mentioned above, the CS in ES is one of the more important factors in helping China to achieve carbon neutrality by 2060. With the support of policy documents such as The Fourteenth Five-Year Plan [8] and the Implementation Plan for Carbon Peaking and Carbon Neutrality Supported by Science and Technology (2022–2030) [11], the accounting of CS in ES has been elevated to the national level. Establishing a more scientific and reasonable accounting system to clarify the interannual variation in ecological spatial carbon sink, and exploring the leading factors affecting this, are very important for accurately predicting the future change of atmospheric CO_2 concentration and formulating targeted policies to consolidate and improve the capacity of CS. Based on China's developmental needs, this study accounted for and analyzed the capacity of CS in CES using refined grid data and explored the leading effects of temperature and precipitation on CS in CES in order to provide scientific and technological support for China's sustainable development and the realization of the "dual carbon" goals.

2.2. Data Analysis

The boundary data used in this study include China's administrative boundaries and the scope of the CES. The vector data of China's administrative boundaries were obtained from the National Administrative Division Information Query Platform, which includes the boundary areas of 34 provinces, municipalities, or special administrative regions in China. (http://xzqh.mca.gov.cn/map (accessed on 24 September 2022)). It is mainly used to analyze the differences of CS in different regions at the administrative unit scale. The scope of CES has been extracted from the multi-period remote sensing monitoring dataset of China's land use/cover changes (CNLUCC), obtained by the Resource and Environmental Science and Data Center of the Chinese Academy of Sciences (https://www.resdc.cn/

(accessed on 24 September 2022)) [33]. The time of the data is 2020, and the spatial resolution of the data is 1000 m × 1000 m, including woodland, shrubland, sparse woodland, other woodland, high-coverage grassland, medium-coverage grassland, low-coverage grassland and other vegetation-covered areas. The dataset is constructed by human–computer interactive visual interpretation. Its basic data is the remote sensing data of Landsat MSS, TM/ETM, and Landsat 8 satellites and supplemented by the charge-coupled device multi-spectral data of China Environment 1 Satellite. In the process of interpretation, Liu et al. [34] referred to the existing grass map, vegetation map, and topographic map to ensure the reliability of the dataset and verified the accuracy of the dataset by randomly sampling the verification line, which reached 95.66%. In addition, before extracting the boundary of CES, the boundaries of forest and grassland were compared between this dataset with the land cover data of Moderate-resolution Imaging Spectroradiometer (MODIS) [35] and global land 30 [36]. It was found that in China, due to the lack of field verification points, the land cover data of MODIS and Global 30 were not well evaluated and corrected. There is a small estimate of the area of ES in China. Therefore, we finally adopted the boundary of CES extraction from CNLUCC.
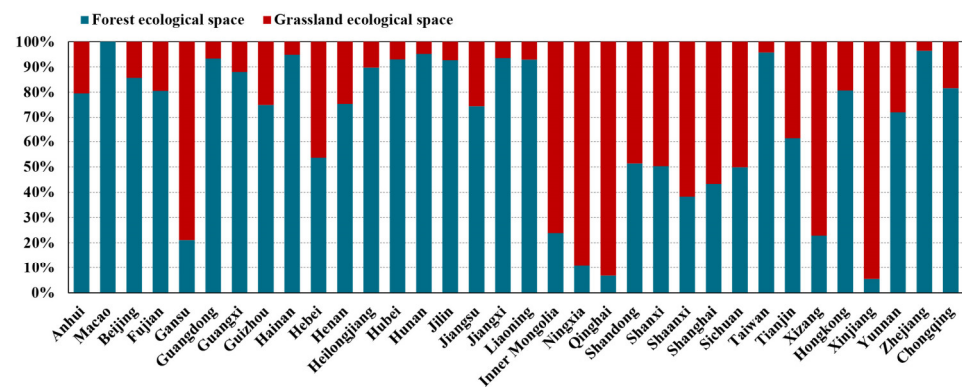

Figure 1. The area proportion of forest ecological space and grassland ecological space in different provinces of China.
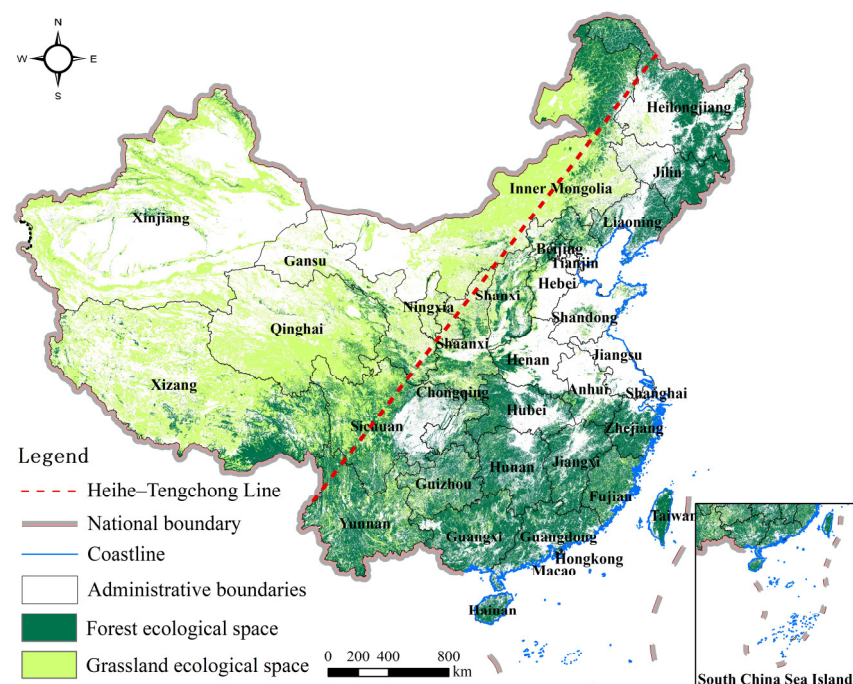

Figure 2. Study area.

In this study, the land surface water index (LSWI), photosynthetically active radiation (PAR), enhanced vegetation index (EVI), temperature and precipitation were obtained by using the Google Earth Engine (GEE), and were used to establish the VPM model to calculate the gross primary productivity (GPP). The calculation results were corrected by the GPP product of MYD17A2H Version 6 [37].

The LSWI was obtained based on surface reflectance data from MOD09A1 Version 6 product [38]. The time period of original surface reflectance data is every 8 days, and the spatial resolution is 500 m × 500 m. The original surface reflectance data was corrected according to atmospheric conditions such as gas, aerosols, and Rayleigh scattering. Based on this surface reflectance data, the LSWI dataset was extracted on GEE platform according to the principle that the absorption of vegetation in near-infrared band is low, but in the short infrared band it is high.

The photosynthetically active radiation (PAR) is an MCD18A2 Version 6.1 product [39]. The data are generated by the Terra and Aqua MODIS combined surface radiation algorithm. The original data was generated by using the multi-temporal characteristics of MODIS data to derive the surface reflectivity. The time period of the data is daily, and the spatial resolution is 5000 m × 5000 m. The data product has been verified in Phase 1.

The enhanced vegetation index (EVI) is calculated from the bidirectional surface reflectance with atmospheric correction provided by MOD13A2 Version 6 product [40]. The time period of the original data is every 16 days, and the spatial resolution is 1000 m × 1000 m. The algorithm of this product would select the best available pixel value from all the collections during the 16-day period, and the standard used is the lowest cloud cover, the lowest viewing angle, and the highest value of EVI, which guarantees the data quality. At the same time, this data also shielded water, clouds, heavy aerosols, and cloud shadows and used blue tape to remove the residual air pollution caused by smoke and sub-pixel thin clouds. The data product has been verified in phase 3, which has high reliability.

The mean temperature and precipitation datasets were obtained from the National Qinghai–Tibet Plateau Scientific Data Center (http://data.tpdc.ac.cn/ (accessed on 24 September 2022)) [41,42]. The spatial resolution is 0.0083333° × 0.0083333° (about 1000 m × 1000 m) and temporal resolution is monthly. This dataset was generated by downscaling the Delta spatial downscaling scheme for China based on the global 0.5° × 0.5° climate dataset published by Custom Resolution Utility (CRU) (The CRU dataset is one of the most widely used climate datasets at present and has relatively accurate assessment results in China. The average mean absolute error (MAE) is 1.598, and the average root mean squared error (RSME) is 1.759. This dataset that has been updated to the version 4. [43]) and the global high-resolution climate dataset published by WorldClim. The dataset was generated in China through the Delta spatial downscaling scheme. In addition, 496 independent meteorological observation point data were used for verification, the verification results show that the MAE and RMSE of the new dataset are all better than the original dataset; that is, the reduced dataset has higher precision than the original CRU dataset, and the verification results can be trusted to have higher reliability for this study [44].

In this study, after all data were acquired, ArcGIS 10.5 software was used for data preprocessing such as unified coordinate system and spatial resolution. All data coordinates have been converted to GCS_WGS_1984. Datum is D_WGS_1984. The Prime Meridian is Greenwich. The Angular Unit is Degree. The spatial resolutions of all the raster data are uniformly 1000 m × 1000 m.

3. Methods

3.1. Research Framework

In this study, the capacity of CS in CES and its dominant influencing factors were calculated through the following steps:

Step 1: The estimation of CS in CES. Based on the VPM model and the soil respiration model, the interannual CS in CES at the grid scale was estimated from 2010 to 2020;

Step 2: Analysis of temporal and spatial variation characteristics of CS in CES. Based on the estimation results of CS in CES at the grid scale, the spatial distribution characteristics and interannual variation trends of CS in CES from 2010 to 2020 were discussed. The spatial variation characteristics of CES at the grid scale were analyzed by constructing a linear regression equation;

Step 3: Stability analysis of CS in CES. By constructing the coefficient of variation equation of CS in CES, the spatial and temporal variation rates of CS in CES at the grid scale were calculated, and the stability of CS in CES were studied;

Step 4: Study of the dominant influencing factors in CES. By calculating the correlation between CS in CES with precipitation and temperature, the influence of temperature and precipitation over CS in CES capacity was explored.

3.2. The Estimation Model of CS

NEP is the net primary productivity (NPP) minus the photosynthetic products consumed by heterotrophic respiration (soil respiration) [45]. NPP represents the fraction of organic carbon fixed by vegetation minus its own respiratory consumption. GPP represents the amount of organic carbon fixed by organisms (mainly green plants) through photosynthesis in unit time, which can be estimated by VPM model [46]. NEP is often used to measure the CS of CES per unit time and area [47]. When NEP > 0, there is a net amount of carbon storage in the ES. When NEP < 0, it indicates that the ES is mainly carbon source. Therefore, the calculating of NEP can accurately measure the carbon budget of ES, which is of great significance to the research of the global carbon cycle and the research of global climate change under the influence of CO_2. In this study, the interannual NEP of CES was estimated by coupling the VPM model [48] with the soil respiration model [49], and the CS in CES was finally obtained on the grid.

$$CS(x,t) = NEP(x,t) \times S$$

$$NEP(x,t) = NPP(x,t) - R_H(x,t)$$

$$NPP(x,t) = GPP(x,t) \times r_{NPP/GPP}$$

where $CS(x,t)$, $NEP(x,t)$, $NPP(x,t)$, $R_H(x,t)$, and $GPP(x,t)$ indicate carbon sink, net ecosystem productivity, net primary production, soil microbial respiration, and gross primary productivity of grid x at time t, respectively. S indicates the area. $r_{NPP/GPP}$ represents the carbon utilization rate, which refers to the efficiency of the vegetation in ES to convert the productivity into biomass and store it in ES. With reference to the research of Chen et al. [50] and Parton et al. [51] the value is 0.55 in this study.

GPP is estimated based on VPM model, and the formula is as follows:

$$GPP(x,t) = \varepsilon \times APAR_{chl}$$

where $APAR_{chl}$ is the photosynthetic effective radiation absorbed by chlorophyll. ε is the actual light energy utilization rate.

$$APAR_{chl} = PAR \times FPAR_{chl}$$

$$FPAR_{chl} = (EVI - 0.1) \times 1.25$$

where PAR is the photosynthetically active radiation. $FPAR_{chl}$ is the proportion of photosynthetic effective radiation absorbed by chlorophyll. EVI is the enhanced vegetation index.

$$\varepsilon = \varepsilon_{max} \times T_{scalar} \times W_{scalar}$$

$$T_{scalar} = \frac{(T - T_{min})(T - T_{max})}{(T - T_{min})(T - T_{max}) - (T - T_{opt})^2}$$

$$W_{scalar} = \frac{1 + LSWI}{1 + LSWI_{max}}$$

where ε_{max} is the maximum utilization rate of light energy. The ε_{max} of FES is 1.106 gC/MJ, and the ε_{max} of GES is 0.608 gC/MJ [52]. T_{scalar} is temperature stress factor. W_{scalar} is water stress factor. T is the temperature. $LSWI$ is the land surface water index.

R_H is estimated by the soil respiration model. The formula is as follows:

$$R_H(x,t) = 0.22 \times (exp(0.0912 \cdot T(x,t)) + ln(0.3145 \cdot P(x,t) + 1)) \times 30 \times 46.5\%$$

where T and P indicate temperature and precipitation, respectively.

3.3. Analysis on Interannual Fluctuation of CS

In this study, the change rates of CS in CES at interannual scales were obtained by calculating the slope of the regression trend line of each grid [53].

$$\theta_{slope} = \frac{n \times \sum_{i=1}^{n} i \times CS_i - \sum_{i=1}^{n} i \cdot \sum_{i=1}^{n} CS_i}{n \times \sum_{i=1}^{n} i^2 - \left(\sum_{i=1}^{n} i\right)^2}$$

where n indicates the number of estimated years. This study covered the period from 2010 to 2020; that is, n is 11. CS_i is the CS of time i. θ_{slope} indicates the trend slope. $\theta_{slope} > 0$ indicates that CS increases gradually over time; otherwise, it decreases gradually. According to the variation trend of θ_{slope}, the CES is divided into five zones: $\theta_{slope} < -5$ is the "significant deterioration zone". $-5 \leq \theta_{slope} < -1$ is the "slight deterioration zone". $-1 \leq \theta_{slope} < 2$ is the "basically stable zone". $2 \leq \theta_{slope} < 6$ is the "slight improvement zone". $\theta_{slope} \geq 6$ is the "significant improvement zone".

3.4. Stability Analysis of CS

In this study, the coefficient of variation was used to analyze the stability of CS at grid scale [54].

$$C_v = \frac{\sigma}{|\overline{x}|}$$

where C_v, σ and $\overline{x}$ indicate the coefficient of variation, standard deviation, and average respectively.

According to the calculation results, the stability of NEP in CES was divided into five levels: $C_v > 5$ is the "highest" variation level. $2.5 < C_v \leq 5$ is a "higher" variation level. $1.5 < C_v \leq 2.5$ is the "medium" variation level. $0.5 < C_v \leq 1.5$ is a "lower" variation level. $0 < C_v \leq 0.5$ is the "lowest" variation level.

3.5. Correlation Analysis between Climate Change and CS

In order to further explore the response relationship between the temporal and spatial variation of CS and climate change, the correlation of CS with temperature and precipitation was established [27].

Correlation coefficient:

$$R_{xy} = \frac{\sum_{i=1}^{n} \left[(x_i - x_p)(y_i - y_p) \right]}{\sqrt{\sum_{i=1}^{n} (x_i - x_p)^2 \sum_{i=1}^{n} (y_i - y_p)^2}}$$

Partial correlation coefficient:

$$R_{xy \cdot z} = \frac{R_{xy} - R_{xz} R_{yz}}{\sqrt{(1 - R_{xz})^2 (1 - R_{yz})^2}}$$

where x_i and x_p indicate the CS and the average CS over many years. y_i and y_p indicate the value and the average value of influencing factors. $r_{xy \cdot z}$ is the partial correlation coefficient between x and y after fixed z.

The *t*-test method was used to test the significance of the correlation coefficient and the partial correlation coefficient. At a confidence level of 0.95, the coefficients were classified as "significant positive correlation", "significant negative correlation", "insignificant positive correlation", and "insignificant negative correlation".

4. Results

4.1. Spatial Distribution of CS in CES

Figure 3 shows the multi-year average NEP of CES on the grid from 2010 to 2020. According to Figure 3, the spatial distribution pattern of the capacity of CS in CES is significantly different. In terms of the types of ES, the CS per unit area of FES is high in eastern and southeastern China, and this advantage is even more pronounced in Heilongjiang, Jilin, and Liaoning, as well as in the intersecting regions of Shaanxi, Hubei, and Henan. The GES is located in the western and northwestern regions of China, although their very wide distribution area contributes greatly to the CS of CES, and the CS per unit area is lower than that in FES. There are still a large number of areas with negative NEP values, meaning that they do not have CS but carbon sources. Specifically, the annual average NEP of CES was 233.78 gC·m^{-2}·a^{-1}, and the annual average CS was 1075.04 TgC/a. Here, the annual average NEP of FES was 255.12 gC·m^{-2}·a^{-1}, and the annual average CS was 499.51 TgC/a. The annual average NEP of GES was 212.45 gC·m^{-2}·a^{-1}, and the annual average CS was 537.52 TgC/a.
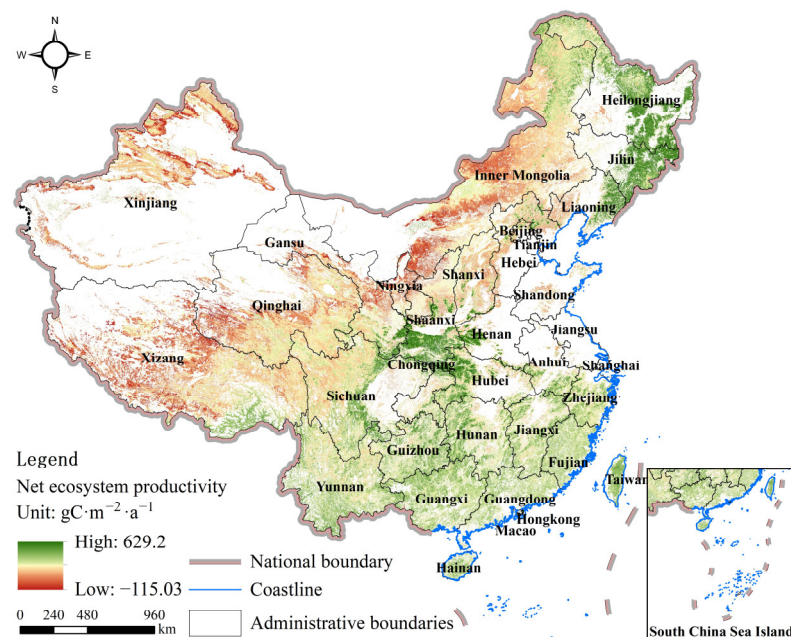

Figure 3. Spatial distribution of multi-year mean NEP in CES.

Figure 4 shows the annual average NEP of ES in different provinces of China. According to Figure 4, in terms of the capacity for CS per unit area in CES, the province with the highest annual mean value of NEP was Taiwan, at 317.41 gC·m^{-2}·a^{-1}. Jilin (309.40 Gc·m^{-2}·a^{-1}) and Chongqing (308.12 Gc·m^{-2}·a^{-1}) followed. These areas are widely distributed with FES, and the strong capacity of CS in FES makes the annual average NEP in these areas high. The lowest NEP is found in Ningxia, with an average of 99.97 Gc·m^{-2}·a^{-1}. Tibet, Inner Mongolia, Xinjiang, Qinghai, and other regions have the lowest average NEP from 2010 to 2020. The main reason for this is that these areas are dominated by GES (the area of GES accounts for 87.96% of the total area of ES), and the capacity for CS in GES is more affected by temperature and precipitation than of FES, resulting in relatively low annual NEP in these areas. Furthermore, Figure 5 shows that the region with the largest annual average CS is Inner Mongolia, whose annual average CS from 2010 to 2020 was

104.37 TgC/a. Tibet (88.10 TgC/a) and Yunnan (75.85 TgC/a) follow. The ES in these regions was huge, especially in Inner Mongolia, where the it covered 880,000 km^2, accounting for 74% of the region's total land area. It can be concluded that for China, it is not only necessary to improve the capacity of CS in ES but also necessary to ensure the area of ES and maintaining the ecological red line, which are of important significance for China's construction of ecological civilization and the realization of the "dual carbon" goals.
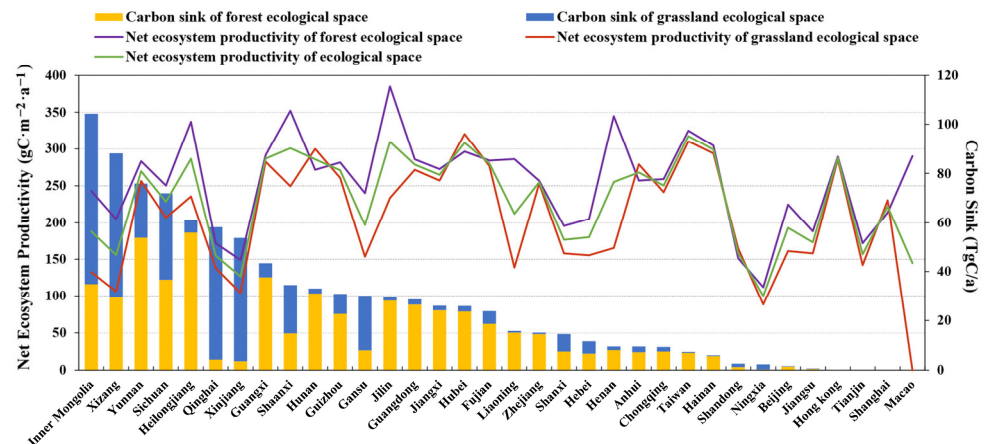

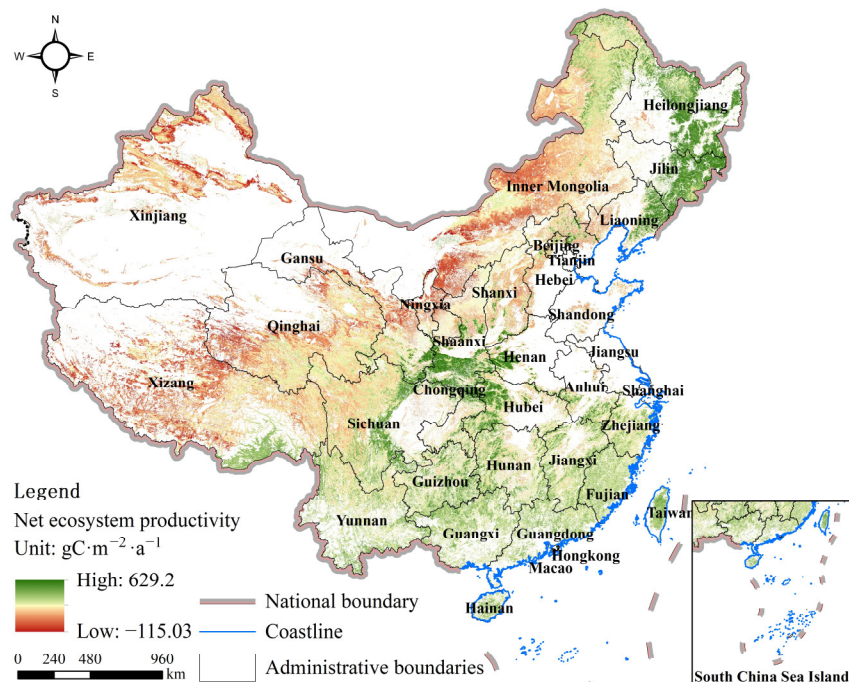**Figure 4.** Average NEP and CS at the provincial scale in China.

Figure 5. Spatial distribution of cumulative NEP of CES.

Figure 5 shows the cumulative NEP of CES from 2010 to 2020. According to Figure 5, the cumulative NEP of CES was 2571.58 Gc·m^{-2}, and the cumulative CS was 11.83 PgC. The cumulative NEP of FES was 2086.18 Gc·m^{-2}, and the cumulative CS was 5.49 PgC. The cumulative NEP of GES was 2336.99 Gc·m^{-2}, and the cumulative CS was 6.33 PgC. According to the cumulative CS of CES from 2010 to 2020, carbon source areas and CS areas were further extracted, as shown in Figure 6. It can be seen from Figure 5 that the CS area (NEP > 0) from 2010 to 2020 was about 4.45 million km^2, accounting for 95.25% of the total area of CES, with a cumulative NEP and CS of 2643.33 Gc·m^{-2} and 12.75 PgC, respectively. The carbon source area (NEP < 0) was about 221,900 km^2, accounting for 4.75% of the total area of CES. The cumulative NEP and CS were −364.12 Gc·m^{-2} and 0.08 PgC, respectively.
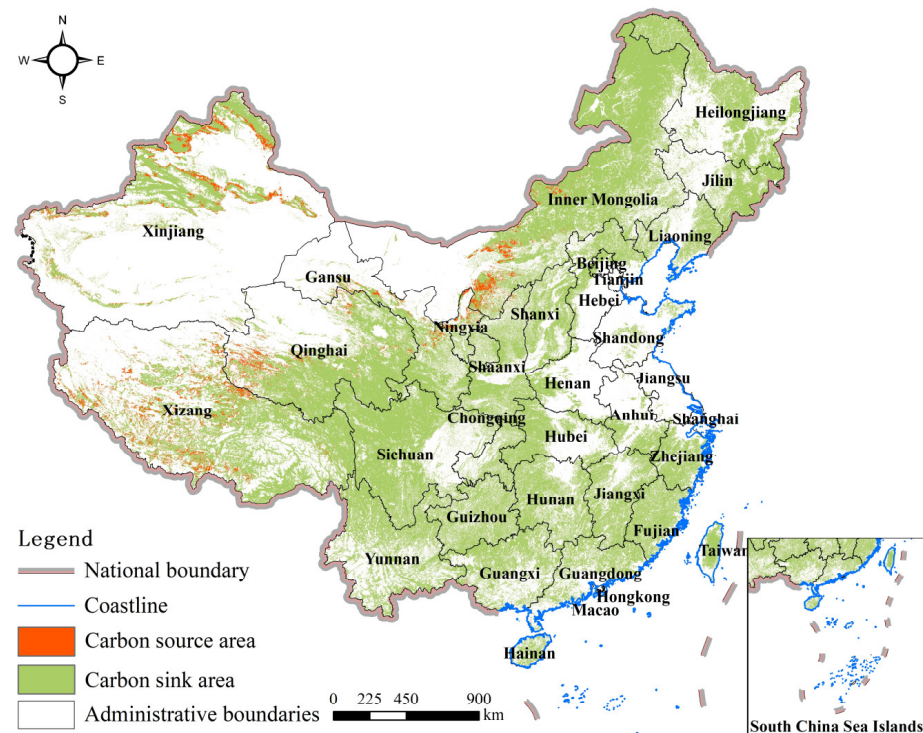
Figure 6. Spatial distribution of carbon source area and CS area in CES.

4.2. Interannual Fluctuation of CS in CES

Figure 7 shows the overall interannual variation trend of NEP and CS in CES from 2010 to 2020. As shown in Figure 7, The annual average NEP and CS of CES fluctuated significantly but generally showed an upward trend. In 2011, the CS in CES was at the lowest level, the NEP was $224.80 \cdot Gc \cdot m^{-2} \cdot a^{-1}$, and the CS was 1049.17 TgC/a. After 2011, the CS in CES gradually fluctuated and increased. In 2019, the CS in CES reached its highest value in nearly 11 years; the NEP was $242.36 \cdot Gc \cdot m^{-2} \cdot a^{-1}$, and the CS was 1131.10 TgC/a. It is worth noting that the NEP and CS in CES decreased significantly in 2014, and then recovered to a pre-decline level. The survey found that the average annual precipitation in the study area was much lower in 2011 and 2014 than in other years. Taking 2014 as an example, the average annual precipitation in the study area was 386.38 mm, and the average annual precipitation was 416.19 mm in 2013 (before NEP and CS went down) and 421.32 mm in 2015 (after NEP and CS went down). Therefore, we suspect that the changes in precipitation play a crucial role in influencing the CS of CES.
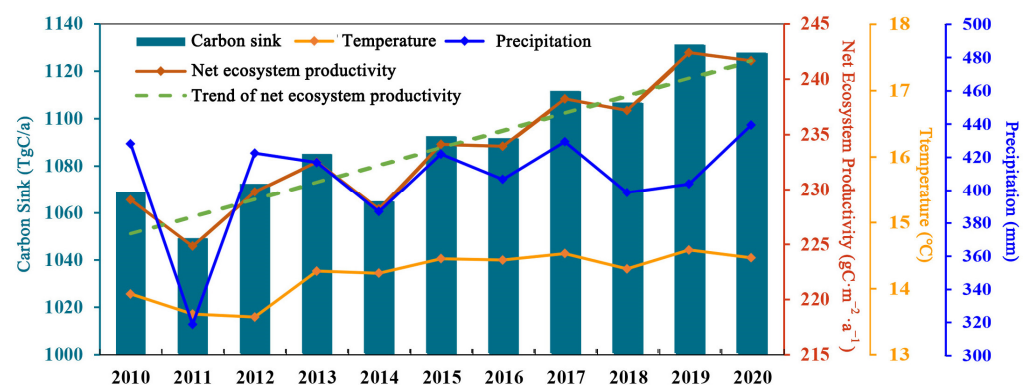

Figure 7. Trends of annual average NEP and CS in CES.

Figure 8 shows the interannual variation rate of CS in CES by grid. As shown in Figure 8, the interannual variation rate of CS in CES is in the obvious improvement zone and the slight improvement zone, accounting for 84.14% and 4.35% of the total area of CES, respectively. The area in the basic stability zone accounts for about 5.47%. The area of deterioration is less than 10%. The area proportion of the significant deterioration zone is about 1.86%, and the area proportion of the slight deterioration zone is about 4.18%. It can be seen that the CS in CES has been significantly improved in recent years, and the overall increase trend is obvious. Further analysis shows that the obvious improvement zone and slight improvement zone are mainly located in the southeast of the country, while the significant improvement zone and slight improvement zone are mainly located in the northwest of the country. This distribution feature is highly consistent with the boundary of the 0 °C isotherm and 400 mm isohyet in China.
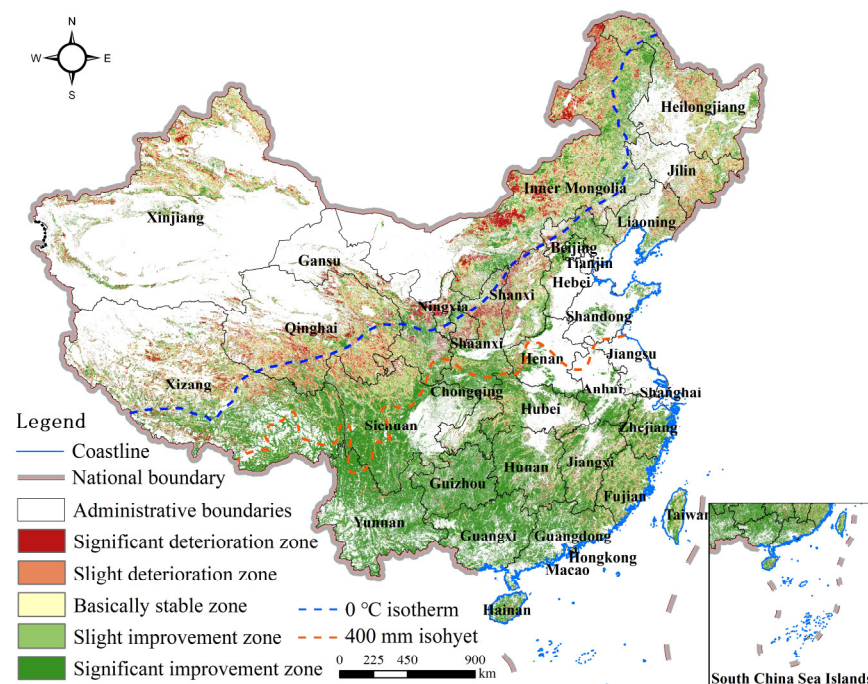

Figure 8. The interannual change rate of CS in CES.

4.3. Spatio-Temporal Stability of CS in CES

The coefficient of variation was further used to measure the stability and volatility of CS in CES. The larger the coefficient of variation is, the more frequently the CS in this region changes, and the more it fluctuates. Figure 9 shows the spatial distribution of the coefficient of variation of CS in CES. As shown in Figure 9, the mean coefficient of variation of CS in CES was 0.6248, generally indicating a relatively stable state. Most areas of CES showed the lowest level of variation, that is, high stability, accounting for about 80.20% of the total area of CES, mainly in the area east of the isohyet line, and the main type of ES was FES. The lower variation and medium variation level accounted for 13.76% and 2.68% of the total area of CES, respectively, and were distributed in the west and around the 400 mm isohyet. The areas with higher and the highest variation level accounted for 1.73% and 1.63% of the total area of CES, respectively. These areas are widely distributed near the 40 mm isohyet, especially the GES in Inner Mongolia. They are jointly affected by climate conditions and human grazing activities, and the CS fluctuates significantly. Therefore, China should focus on these regions to achieve the goal of improving the quality of CES and capacity of CS in CES.
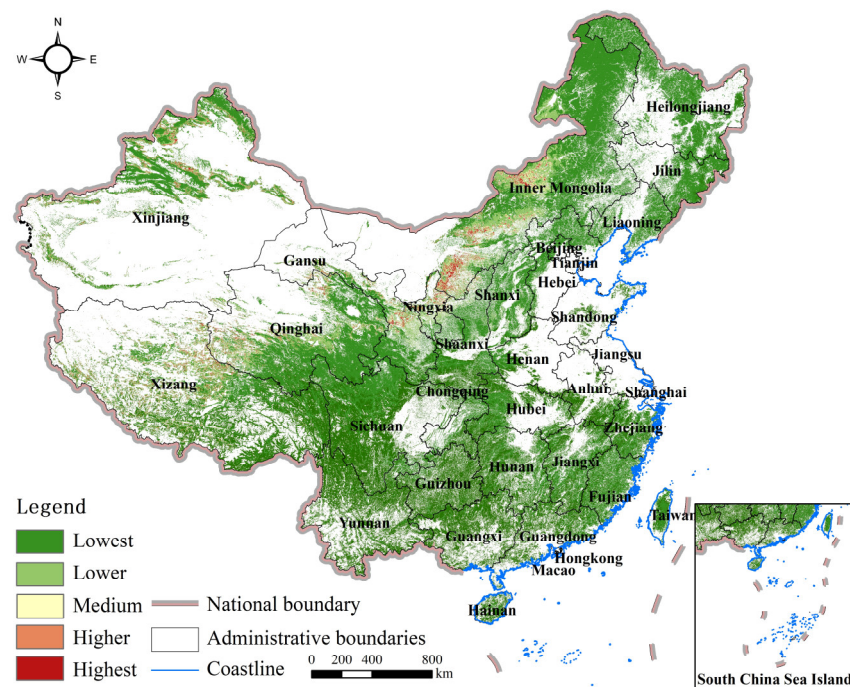
Figure 9. Spatio-temporal stability of CS in CES.

4.4. Dominant Factors Analysis of CS in CES

Figure 10 shows the correlation coefficient of CS in CES with temperature and precipitation. As shown in Figure 10, the CS in CES is highly positively correlated with precipitation change, with an average correlation coefficient of 0.085. The area showing a significant positive correlation between CS and precipitation accounted for 53.12% of the total CES area, and these areas were widely distributed in the whole area of CES. The area with the most significant negative correlation between CS and precipitation accounted for 25.49%, and these regions were highly coincident with the regions with low spatio-temporal stability, as described above, and were located around the 400 mm isohyet of China. The areas showing significant positive correlation between CS and temperature accounted for 41.63% of the total CES area, and the distribution area was relatively scattered, indicating that the promotional effect of temperature on CS in CES was obviously weaker than that of precipitation. The areas showing a negative correlation between CS and temperature accounted for 32.37% of the total area of CES. They were distributed in a concentrated way, and mostly located in GES. This may be due to the fact that temperature rise leads to an unsynchronized water and heat demand for vegetation growth in grassland, which inhibits the CS of grassland to a certain extent [29].

Figure 11 shows the partial correlation coefficient of CS in CES with temperature and precipitation. The partial correlation analysis between CS and precipitation shows that the proportion of significant positive correlation area increased to 62.58% of the total area of CES, while the proportion of insignificant correlation area decreased significantly. This further verifies the positive role of precipitation in promoting CS in CES. However, the weak promoting effect of temperature and the large range of consistent effects, to a certain extent, affect the response process of CS to precipitation. The partial correlation analysis of CS and temperature shows that the proportions of significant positive correlation and significant negative correlation areas decreased significantly, accounting for about 36.84% and 22.53% of the total area of CES, respectively, while the insignificant correlation areas increased to a large area. In general, precipitation and temperature jointly affect the CS in CES, but the influence of temperature on CS in CES is weaker than that of precipitation, with primarily a weak positive correlation, or even a large range of negative correlation. The influence of precipitation on CS in CES is mainly positive. Under the coupling effect dominated by precipitation, they jointly promoted the gradual increase in CS in CES.
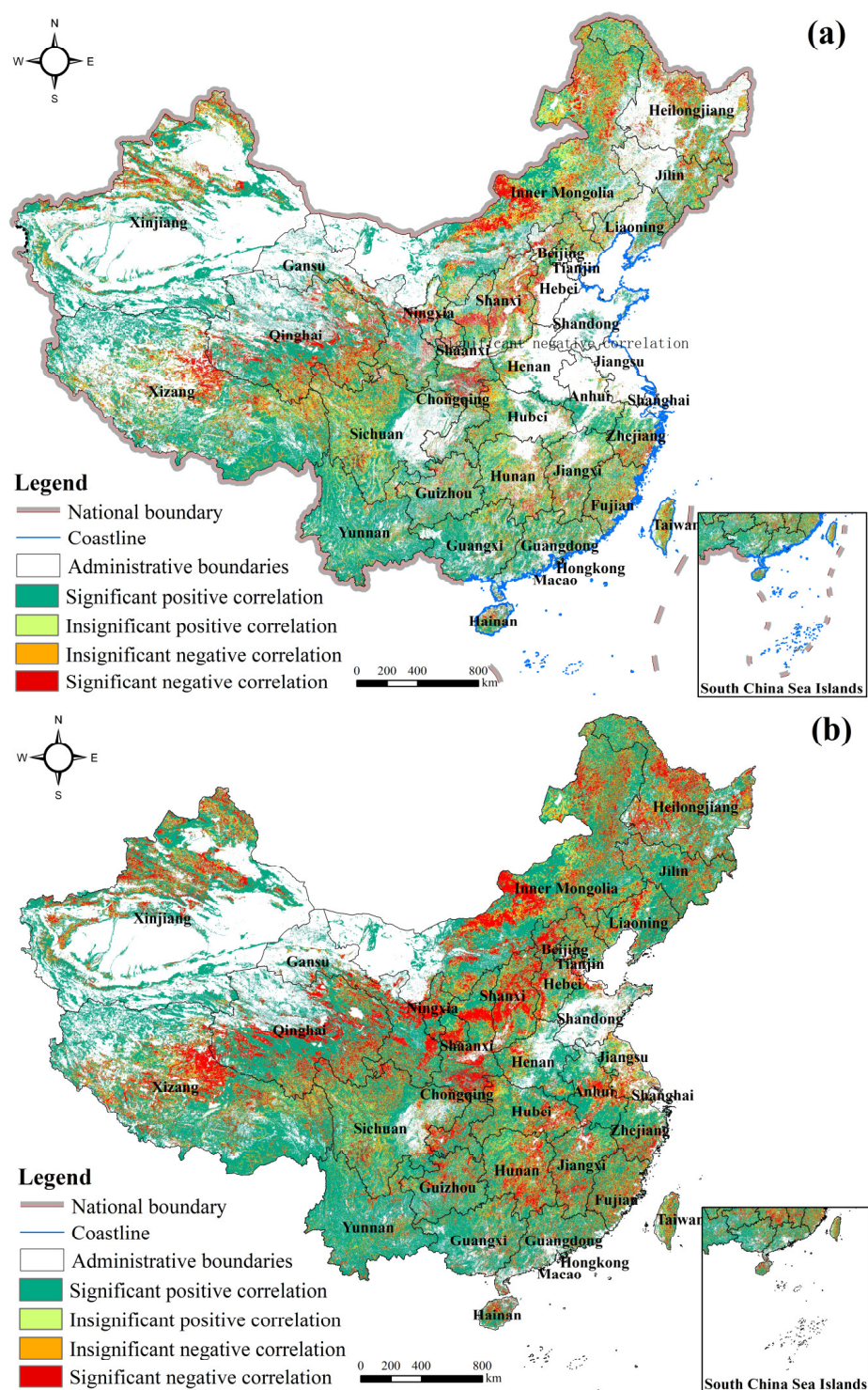
Figure 10. Correlation of CS in CES with (**a**) temperature and (**b**) precipitation.
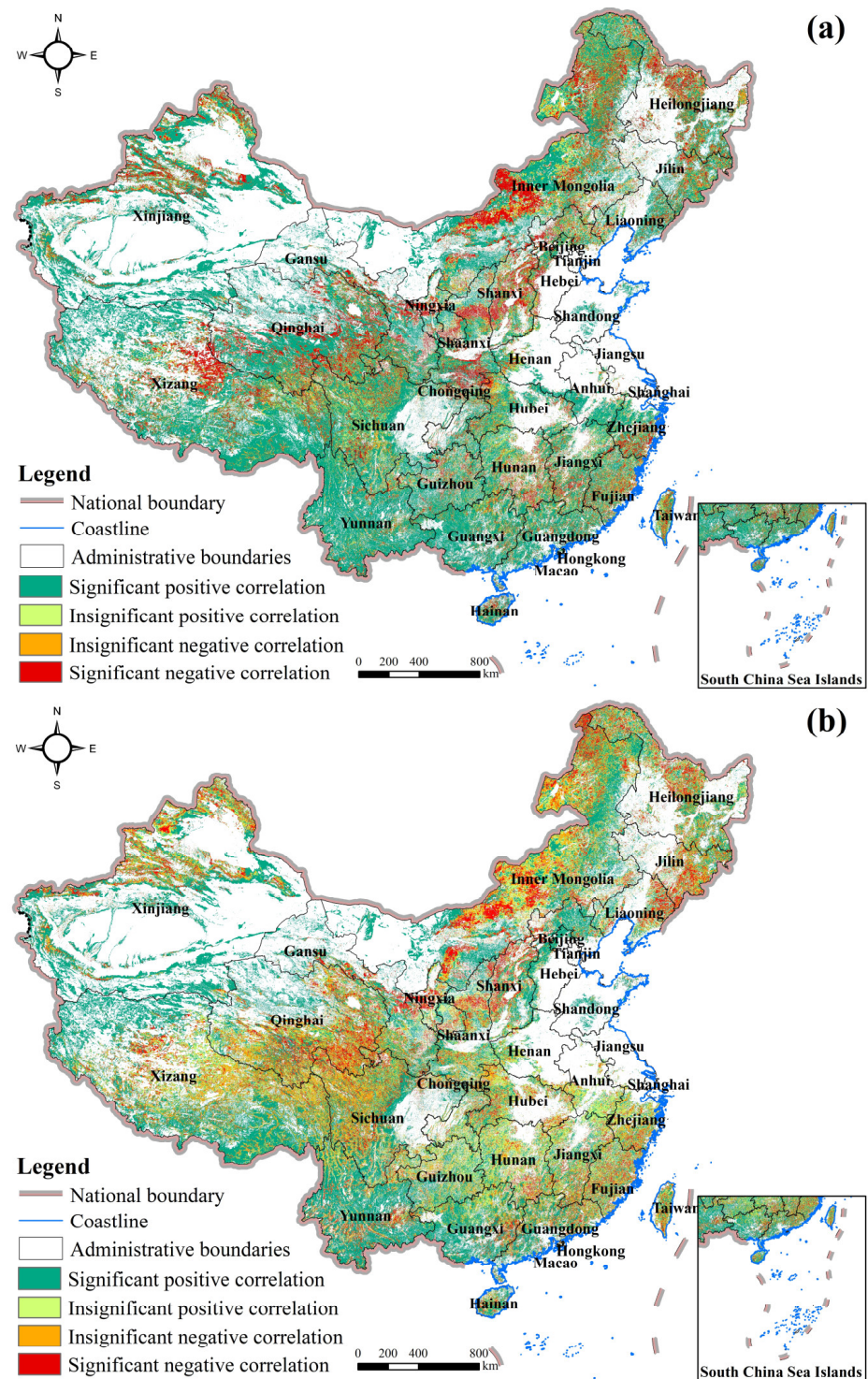
Figure 11. Partial correlation of CS in CES with (**a**) temperature and (**b**) precipitation.

5. Discussion

Guided by national needs, this study has established a grid-scale-based accounting method for carbon sink (CS) in Chinese ecological space (CES), assessed the capacity of CS in CES and discussed the impact of climate factors on CS in CES. The results show that the multi-year average CS in CES per unit of time and area was 233.78 Gc·m^{-2}·a^{-1}, and the multi-year cumulative CS was 11.83 PgC, including 5.49 PgC CS in forest ecological space (FES) and 6.33 PgC CS in grassland ecological space (GES). It should be noted that, in terms of per unit area, the capacity of CS in FES is higher than that in FES, with values of

255.12 Gc·m^{-2}·a^{-1} and 212.45 Gc·m^{-2}·a^{-1}, respectively. This may be because the capacity of CS in GES is far more affected by temperature and precipitation than that in FES. At the same time, there were still many areas where the GES was a carbon source area, but its very wide distribution area has contributed more to the CS of CES, and the total CS of GES was greater than the total CS of FES.

The study further determined the carbon source area and CS area of CES, which were 12.75 PgC and −0.08 PgC, respectively. The analysis of the time change trends of CS in CES shows that the total amount of CS trended upward from 2010 to 2020, but it was extremely low in 2011 and 2014. The statistical results of precipitation show that the annual average precipitation in these 2 years was far lower than that in other years, which confirms that the change in precipitation has a significant impact on the CS of CES. This may have been caused by the decrease in precipitation, which led to a decrease in CES distribution area and the weakening of soil respiration, thus causing the decrease in CS. The results of the temporal and spatial variation trend of CS in CES on the grid scale show that the boundaries at which the capacity of CS in CES becomes better and worse are highly correlated with the boundary lines of China's 0 °C isotherm and 400 mm isohyet. Specifically, 'the regions to the south of the 0 °C isotherm and 400 mm isohyet, driven by high precipitation, gradually evolve towards a better capacity of CS. However, in the area north of the 0 °C isotherm and 400 mm isohyet, the capacity of CS fluctuates significantly, and gradually becomes worse under the influence of climate factors. In addition, this study also analyzed the stability of CS in CES. The average variation coefficient of CS in CES is 0.6248, which generally indicates a relatively stable state. However, there are areas with higher variability, and the highest variability is found near the 400 mm isohyet, which mainly focuses on GES, further verifying that GES is greatly affected by temperature and precipitation.

In this study, in order to further explore the dominant influencing factors of the fluctuation of CS in CES, the correlation of CS in CES on precipitation and temperature were calculated. The results show that CS in CES was positively correlated with precipitation, with an average correlation coefficient of 0.085. Temperature showed a weak positive correlation, with an average correlation coefficient of 0.026. When one factor was kept unchanged, the results of the partial correlation coefficient show that precipitation and temperature jointly affected the CS of CES within the given climate environment, but this effect was dominated by precipitation. In addition, there were large areas of overlap between regions showing a significant negative correlation between CS and temperature and regions showing significant negative correlation between CS and precipitation in CES. Under the influence of multi-variable climate conditions, the fluctuation was less affected by climate conditions and more likely depended on the ecological service regulation ability of itself and its response degree to the change of atmospheric CO_2 concentration [28].

In short, this study has established a grid-scale estimation model for the CS in CES. Based on the detailed analysis of the spatio-temporal evolution characteristics and stability of CS in CES, the influence of precipitation and temperature on the change of CS in CES was discussed, and their dominant positions were analyzed. The ideas and results of this study provide a new direction in the planning and optimization of "production–living–ecological" space (PLES) in China, focusing not only on the optimization of land use but also on improving the quality of the interior space so as to promote the gradual transformation of PLES in a more coordinated and sustainable direction. At the same time, the study also provides a direction for the realization of China's Sustainable Development Goals (SDGs) and carbon peak and neutrality ("dual carbon" goals). Although studies on the interannual scale can reveal the correlation of temperature and precipitation changes with CS to a certain extent, this process ignores the impact of different seasonal changes on CS. Andrew et al. [55] have shown that the phenological transition in spring and autumn has a significant positive impact on NEP. The research of Wang et al. [25] also shows that spring warming promotes CS, while summer warming inhibits CS. These studies all show that seasonal change has a significant impact on the CS of ecological space (ES), confirming the results of this study. However, as far as the CS in CES is concerned, the accuracy of their

research results is lacking at the macro level. Therefore, it is necessary to carry out studies at the fine-grid scale (1000 m × 1000 m, or more fine), which can help us to more deeply understand the contribution mechanism of the increasing and decreasing sources of the CES carbon cycle and support the realization of China's "dual carbon" goals with more accurate data. In addition, the impact of land use change and use pressure through time on CS in ES, and the CS of finer categories under FES and GES are not considered in this study, which will also be the focus of future work.

6. Conclusions

Based on a grid-scale accounting method for carbon sink (CS) in Chinese ecological space (CES), this study estimated the CS of CES from 2010 to 2020, and discussed its spatio-temporal change characteristics. The results show that the potential of CS in CES is huge. From 2010 to 2020, the multi-year average CS per unit area was 233.78 Gc·m^{-2}·a^{-1}, and the cumulative CS was 11.83 PgC. In terms of unit area, the capacity of CS in forest ecological space (FES) was higher than that of grassland ecological space (GES) (255.12 Gc·m^{-2}·a^{-1} and 212.45 G Gc·m^{-2}·a^{-1}, respectively). As the area of GES was much larger than that of GES, the CE contribution of GES was generally larger than that of FES. Some GES was affected by climate conditions. The research results show that their location belongs to the carbon source area, with a total area of 22,1900 km^2. The focus should be on improving and optimizing the quality of the interior space so as to realize a transformation from source to sink. The results of the spatio-temporal change trend and stability of CS in CES show that the NEP and CS were, for many years, generally increasing, and were in a relatively stable state (coefficient of variation is 0.6248). The study found that the GES was greatly affected by environmental factors such as precipitation, which led to a lower level of CS in CES in years with low annual precipitation, as well as significant differences in the stability of CS in the ecological space (ES) on the east and west sides of the 400 mm isohyet (taken as the separation line). Further, the analysis of the correlation of CS in CES with precipitation and temperature also confirmed the above. The correlation coefficients of precipitation and temperature with CS in CES were 0.085 and 0.026, respectively. Precipitation plays a major positive role in promoting CS in CES, while temperature plays a weak role, and may even inhibit it. The overall fluctuation of CS in CES is the result of their coupling effect within a climate environment where precipitation is the leading factor. This study provides a new way of thinking regarding the internal optimization and quality improvement of CES and provides technical support for decision-making departments to improve the capacity of CS in ES. The research is of great significance in achieving China's carbon peak and neutrality ("dual carbon" goals) and Sustainable Development Goals (SDGs).

Author Contributions: Conceptualization, G.L. and D.J.; methodology, X.L.; software, X.L.; validation, X.L. and J.F.; formal analysis, G.L.; investigation, X.L.; resources, D.J.; data curation, X.L.; writing—original draft preparation, G.L. and X.L.; writing—review and editing, D.J. and J.F.; visualization, X.L.; supervision, G.L.; project administration, X.L.; funding acquisition, G.L. and J.F. All authors have read and agreed to the published version of the manuscript.

References

1. Zhang, X.P.; Cheng, X.M. Energy Consumption, Carbon Emissions, and Economic Growth in China. *Ecol. Econ.* **2009**, *68*, 2706–2712. [CrossRef]
2. Mekonnen, M.M.; Hoekstra, A.Y. Four Billion People Facing Severe Water Scarcity. *Sci. Adv.* **2016**, *2*, e1500323. [CrossRef] [PubMed]
3. Saier, M.H. Climate Change, 2007. *Water Air Soil Pollut.* **2007**, *181*, 1–2. [CrossRef]
4. Solomon, S.; Plattner, G.K.; Knutti, R.; Friedlingstein, P. Irreversible climate change due to carbon dioxide emissions. *Proc. Natl. Acad. Sci. USA* **2009**, *106*, 1704–1709. [CrossRef]
5. Sanders, S. *125 Questions: Exploration and Discovery*; Science, AAAS Custom Publishing Office: Washington, DC, USA, 2021.
6. Transforming Our World: The 2030 Agenda for Sustainable Development. Available online: https://sdgs.un.org/2030agenda (accessed on 8 May 2022).
7. Action Plan for Carbon Dioxide Peaking Before 2030. Available online: https://www.gov.cn/zhengce/content/2021-10/26/content_5644984.htm (accessed on 8 May 2022).
8. The 14th Five Year Plan for National Economic and Social Development of the People's Republic of China and the Outline of Long-Term Objectives for 2035. Available online: http://www.gov.cn/xinwen/2021-03/13/content_5592681.htm (accessed on 8 May 2022).
9. Schleussner, C.F.; Lissner, T.K.; Fischer, E.M.; Wohland, J.; Perrette, M.; Golly, A.; Rogelj, J.; Childers, K.; Schewe, J.; Frieler, K.; et al. Differential climate impacts for policy-relevant limits to global warming: The case of 1.5 °C and 2 °C. *Earth Syst. Dyn.* **2016**, *7*, 327–351. [CrossRef]
10. Strive to Achieve Carbon Peak by 2030 and Carbon Neutrality by 2060—Win the Hard Battle of Low-Carbon Transformation. Available online: https://www.gov.cn/xinwen/2021-04/02/content_5597403.htm (accessed on 8 May 2022).
11. Notice of the Ministry of Science and Technology and Other Nine Departments on the Issuance of the Implementation Plan for Science and Technology to Support Carbon Peak and Carbon Neutralization (2022–2030). Available online: https://www.gov.cn/zhengce/zhengceku/2022-08/18/content_5705865.htm (accessed on 8 May 2022).
12. Zhao, Y.; Lin, G.; Jiang, D.; Fu, J.Y.; Li, X. Low-Carbon Development from the Energy-Water Nexus Perspective in China's Resource-based city. *Sustainability* **2022**, *14*, 11869. [CrossRef]
13. Li, X.; Dong, D.; Lin, G.; Yan, R.; Li, S. Water Use for Energy Production and Conversion in Hebei Province, China. *Front. Energy Res.* **2020**, *8*, 558536. [CrossRef]
14. Li, Z.; Cai, Y.P.; Lin, G. Pathways for sustainable municipal energy systems transition: A case study of Tangshan, a resource-based city in China. *J. Clean. Prod.* **2022**, *330*, 129835. [CrossRef]
15. Liu, Z.; Guan, D.; Crawford-Brown, D.; Zhang, Q.; He, K.B.; Liu, J.G. Energy policy: A low-carbon road map for China. *Nature* **2013**, *500*, 143–145. [CrossRef]
16. Huang, Y.; Sun, W.J.; Qin, Z.C.; Zhang, W.; Yu, Y.Q.; Li, T.T.; Zhang, Q.; Wang, G.C.; Yu, L.F.; Wang, Y.J.; et al. The role of China's terrestrial carbon sequestration 2010–2060 in offsetting energy-related CO_2 emissions. *Natl. Sci. Rev.* **2022**, *9*, nwac057. [CrossRef]
17. Yu, Z.; Ciais, P.; Piao, S.L.; Houghton, R.A.; Lu, C.Q.; Tian, H.Q.; Agathokleous, E.; Kattel, G.R.; Sitch, S.; Goll, D.; et al. Forest expansion dominates China's land carbon sink since 1980. *Nat. Commun.* **2022**, *13*, 5374. [CrossRef] [PubMed]
18. Liu, Z.; Guan, D.; Moore, S.; Lee, H.; Su, J.; Zhang, Q. Climate policy: Steps to China's carbon peak. *Nature* **2015**, *522*, 279–281. [CrossRef] [PubMed]
19. Wu, Z.Y. "Production-living-ecological" space optimization and Beijing-Tianjin-Hebei ecological environment protection. *City* **2014**, *12*, 26–29.
20. Dybala, K.E.; Steger, K.; Walsh, R.G.; Smart, D.R.; Gardali, T.; Seavy, N.E. Optimizing carbon storage and biodiversity co-benefits in reforested riparian zones. *J. Appl. Ecol.* **2019**, *56*, 343–353. [CrossRef]
21. Zhu, L. *China's Carbon Emissions Report 2016*; Harvard Kennedy School Belfer Center for Science and International Affairs: Cambridge, MA, USA, 2016.
22. Liang, D.; Lu, X.; Zhuang, M.; Shi, G.; Hu, C.Y.; Wang, S.X.; Hao, J.M. China's greenhouse gas emissions for cropping systems from 1978–2016. *Sci. Data* **2021**, *8*, 171. [CrossRef]
23. Friedlingstein, P.; O'Sullivan, M.; Jones, M.W.; Andrew, R.M.; Hauck, J.; Olsen, A.; Peters, G.P.; Peters, W.; Pongratz, J.; Sitch, S.; et al. Global Carbon Budget 2020. *Earth Syst. Sci. Data* **2020**, *12*, 3269–3340. [CrossRef]
24. Ding, G.R.; Zhu, J.X.; Xu, L.; He, N.P. Technological Approaches to Enhance Ecosystem Carbon Sink in China: Nature-based Solutions. *Bull. Chin. Acad. Sci.* **2022**, *37*, 490–501.
25. Wang, K.; Bastos, A.; Ciais, P.; Wang, X.; Rödenbeck, C.; Gentine, P.; Chevallier, F.; Humphrey, V.W.; Huntingford, C.; O'Sullivan, M.; et al. Regional and Seasonal Partitioning of Water and Temperature Controls on Global Land Carbon Uptake Variability. *Nat. Commun.* **2022**, *13*, 3469. [CrossRef]
26. Zhang, T.; Zhang, Y.; Xu, M.; Xi, Y.; Zhu, J.; Zhang, X.; Wang, Y.; Li, Y.; Shi, P.; Yu, G.; et al. Ecosystem Response More than Climate Variability Drives the Inter-Annual Variability of Carbon Fluxes in Three Chinese Grasslands. *Agric. For. Meteorol.* **2016**, *225*, 48–56. [CrossRef]
27. Liu, F.; Zeng, Y.N. Analysis of the spatio-temporal variation of vegetation carbon source/sink in Qinghai Plateau from 2000–2015. *Acta Ecol. Sin.* **2021**, *41*, 5792–5803.

28. Major Data Results of the Third National Land Survey Were Released. Available online: http://www.gov.cn/xinwen/2021-08/26/content_5633497.htm (accessed on 24 September 2022).

29. Hu, H.Y. Population distribution in China with statistical tables and density maps. *Acta Geogr. Sin.* **1935**, *2*, 33–74.

30. Hu, H.Y. The distribution, regionalization and prospects of China's population. *Acta Geogr. Sin.* **1990**, *2*, 139–145.

31. Ding, Y.; Chun, L.; Sun, J.J.; Wu, Z.N.; Yun, X.J.; Li, F.; Jia, D.Z.; Lai, Y.N. China Grassland. *For. Hum.* **2020**, *Z1*, 20–39; + 12–19.

32. Chen, J.; Ding, K. The Diversity of Chinese Forests. *For. Hum.* **2022**, *8*, 14–29.

33. Xu, X.L.; Liu, J.Y.; Zhang, S.W.; Li, R.D.; Yan, C.Q.; Wu, S.X. Multi Period Remote Sensing Monitoring Data Set of Chinese Land Use and Land Cover. Resource and Environmental Science Data Registration and Publishing System. 2018. Available online: https://doi.org/10.12078/2018070201 (accessed on 24 September 2022).

34. Liu, J.; Kuang, W.; Zhang, Z.; Xu, X.; Qin, Y.; Ning, J.; Zhou, W.; Zhang, S.; Li, R.; Yan, C.; et al. Spatiotemporal characteristics, patterns and causes of land-use changes in China since the latce 1980s. *J. Geogr. Sci.* **2014**, *24*, 195–210. [CrossRef]

35. Friedl, M.; Sulla-Menashe, D. MCD12Q1 MODIS/Terra+Aqua Land Cover Type Yearly L3 Global 500m SIN Grid V006. 2019. Distributed by NASA EOSDIS Land Processes DAAC. Available online: https://doi.org/10.5067/MODIS/MCD12Q1.006 (accessed on 11 October 2022).

36. Chen, J.; Ban, Y.; Li, S. China: Open access to Earth land-cover map. *Nature* **2014**, *514*, 434.

37. Running, S.; Mu, Q.; Zhao, M. MYD17A2H MODIS/Aqua Gross Primary Productivity 8-Day L4 Global 500 m SIN Grid V006. Available online: https://doi.org/10.5067/MODIS/MYD17A2H.006 (accessed on 24 September 2022).

38. Vermote, E. MOD09A1 MODIS/Terra Surface Reflectance 8-Day L3 Global 500 m SIN Grid V006. Available online: https://doi.org/10.5067/MODIS/MOD09A1.006 (accessed on 24 September 2022).

39. Wang, D. MODIS/Terra+Aqua Photosynthetically Active Radiation Daily/3-Hour L3 Global 1 km SIN Grid V061. Available online: https://doi.org/10.5067/MODIS/MCD18A2.061 (accessed on 24 September 2022).

40. Didan, K. MOD13A2 MODIS/Terra Vegetation Indices 16-Day L3 Global 1 km SIN Grid V006. Available online: https://doi.org/10.5067/MODIS/MOD13A2.006 (accessed on 24 September 2022).

41. Peng, S. 1-km Monthly Precipitation Dataset for China (1901–2020). National Tibetan Plateau Data Center, 2020. Available online: https://doi.org/10.5281/zenodo.3185722 (accessed on 24 September 2022).

42. Peng, S. 1-km Monthly Mean Temperature Dataset for China (1901–2020). National Tibetan Plateau Data Center, 2019. Available online: https://doi.org/10.11888/Meteoro.tpdc.270961 (accessed on 24 September 2022).

43. Harris, I.; Osborn, T.J.; Jones, P.; Lister, D. Version 4 of the CRU TS monthly high-resolution gridded multivariate climate dataset. *Sci. Data* **2020**, *7*, 109. [CrossRef]

44. Peng, S.; Ding, Y.; Liu, W.; Li, Z. 1 km Monthly Temperature and Precipitation Dataset for China from 1901 to 2017. *Earth Syst. Sci. Data* **2019**, *11*, 1931–1946. [CrossRef]

45. Woodwell, G.M.; Whittaker, R.H.; Reiners, W.A.; Likens, G.E.; Delwiche, C.C.; Botkin, D.B. The Biota and the World Carbon Budget: The Terrestrial Biomass Appears to Be a Net Source of Carbon Dioxide for the Atmosphere. *Science* **1978**, *199*, 141–146. [CrossRef]

46. Fang, J.; Ke, J.; Tang, Z.; Chen, A. Implications and estimations of four terrestrial productivity papameters. *Chin. J. Plant Ecol.* **2001**, *4*, 414–419.

47. Huang, X.J.; Zhang, X.Y.; Lu, X.H.; Wang, P.Y.; Qin, J.Y.; Jiang, Y.C.; Liu, Z.M.; Wang, Z.; Zhu, A.X. Land development and utilization for carbon neutralization. *J. Nat. Resour.* **2021**, *36*, 2995–3006. [CrossRef]

48. Wang, M.M.; Wang, S.Q.; Wang, J.B.; Yan, H.; Mickler, R.A.; Shi, H.; He, H.L.; Huang, M.; Zhou, L. Detection of Positive Gross Primary Production Extremes in Terrestrial Ecosystems of China During 1982–2015 and Analysis of Climate Contribution. *J. Geophys. Res. Biogeosci.* **2018**, *123*, 2807–2823. [CrossRef]

49. Tang, X.; Fan, S.; Qi, L.; Guan, F.; Du, M.; Zhang, H. Soil respiration and net ecosystem production in relation to intensive management in Moso bamboo forests. *Catena* **2016**, *137*, 219–228. [CrossRef]

50. Chen, Z.; Yu, G. Advances in the soil microbial carbon use efficiency. *Acta Ecol. Sin.* **2020**, *40*, 756–767.

51. Parton, W.J.; Schimel, D.S.; Cole, C.V.; Ojima, D.S. Analysis of factors controlling soil organic matter levels in great plains grasslands. *Soil Sci. Soc. Am. J.* **1987**, *51*, 1173–1179. [CrossRef]

52. Running, S.W.; Thornton, P.E.; Nemani, R.; Glassy, J.M. Global terrestrial gross and net primary productivity from the earth observing system. *Methods Ecosyst. Sci.* **2000**, *03*, 44–57.

53. Wang, Q.; Zhang, T.B.; Yi, G.H.; Chen, T.T.; Bie, X.J.; He, Y.X. Tempo-spatial variations and driving factors analysis of net primary productivity in the Hengduan mountain area from 2004 to 2014. *Acta Ecol. Sin.* **2017**, *37*, 3084–3095.

54. Pan, J.H.; Huang, K.J.; Li, Z. Spatio-temporal variation in vegetation net primary productivity and its relationship with climatic factors in the Shule River basin from 2001 to 2010. *Acta Ecol. Sin.* **2017**, *37*, 1888–1899. [CrossRef]

55. Richardson, A.D.; Andy Black, T.; Ciais, P.; Delbart, N.; Friedl, M.A.; Gobron, N.; Hollinger, D.Y.; Kutsch, W.L.; Longdoz, B.; Luyssaert, S.; et al. Influence of Spring and Autumn Phenological Transitions on Forest Ecosystem Productivity. *Philos. Trans. R. Soc. B Biol. Sci.* **2010**, *365*, 3227–3246. [CrossRef]